Pricing and Distributed Scheduling Framework of Multi-microgrid System Based on Coupled Electricity−Carbon Market

Tao Niu, Haoran Li, Guanhong Chen, Sidun Fang, and Ruijin Liao

Abstract—**This paper presents a holistic pricing and distributed scheduling framework for multi-microgrid system (MMGS) that considers the supply−demand relationships of the coupled electricity–carbon market to promote collaborative market trading within the MMGS for economic and environmental benefit improvement. Initially, an operation model of each microgrid is developed by synthetically considering electricity−carbon operational constraints related to generation units and energy storage units. Then, a collaborative optimization strategy of the MMGS is established according to the Nash bargaining game (NBG) model with the objective of maximizing overall operational revenue. To determine the trading schedule, an accelerated prediction-correction-based alternating direction method of multipliers (PCB-ADMM) algorithm is employed to derive the optimal scheduling strategy of MMGS in a distributed manner, ensuring the privacy preservation of individual microgrids. For electricity−carbon pricing, a supply−demand ratio (SDR) based pricing strategy is proposed to dynamically update electricity and carbon allowance prices, which fundamentally guides and incentivizes each microgrid to trade within the MMGS preferentially rather than with an upstream distribution network. Finally, a study case verifies the effectiveness of the proposed framework in enhancing the operation economy and environmental friendliness of the entire MMGS.**

Index Terms—**Electricity market, carbon allowance market, distributed optimization, microgrid, Nash bargaining game, alternating direction method of multipliers (ADMM), distributed scheduling.**

I. Introduction

To achieve the ultimate goal of “carbon peak and carbon neutrality” in the energy industry, various countries worldwide have placed increasing emphasis on the “safety, efficiency, cleanliness, and low-carbon” operation [1], [2] of electric power systems. A microgrid (MG), which locally coordinates and regulates a series of distributed energy sources and loads, is considered an essential component of future distribution systems [3], [4]. In addition, traditional MGs tend to adopt a centralized energy scheduling and trading scheme, where insufficient or excessive electricity can be balanced only through transactions with upstream distribution network. In this case, MGs can only passively accept trading prices assigned by upstream distribution network; thus, it is imperative to develop an elastic marketization mechanism to effectively incentivize MGs to engage in energy sharing [5].

To address this issue, the concept of a multi-microgrid system (MMGS) has been proposed to form a functionally interactive and mutualistic subsystem comprising a group of networked MGs. Owing to flexible power and information exchange among networked MGs, the collaboration of multiple MGs not only enhances operational stability and reliability, but also creates space for additional economic revenue by fully utilizing the idle capacity of each MG [6]. The development of the MMGS platform fosters direct information and energy exchange among MGs, which further introduces a market-based peer-to-peer (P2P) energy trading scheme and increases MG revenue [7].

Many studies have investigated the scheduling and pricing strategies of MMGS, as shown in Table I, where SDR stands for supply−demand ratio. The existing scheduling strategies for MMGS can be classified into two categories, game-based and nongame-based, with the game-based strategies further divided into cooperative and noncooperative games. In the nongame-based scheduling strategies, [8] aimed to minimize the annual total cost in multiple scenarios, accounting for the power exchange among MGs. This strategy significantly reduced the total costs and achieved the global optimality. However, it employed a centralized optimization approach, overlooking the privacy and security requirements of individual MGs. As an improvement, distributed decision methods have been explored and adopted in many works, where the alternating direction method of multipliers (ADMM) was widely utilized [9]-[11], effectively ensuring privacy protection requirements while minimizing the total operation costs of the entire system. In fact, as a rational and autonomous participant in an MMGS, each MG would be unwilling to cooperate if its own benefits were sacrificed compared with those of independent operation. To promote cooperation and coordination among MGs, some studies have es-

Manuscript received: March 15, 2024; revised: June 24, 2024; accepted: September 3, 2024. Date of CrossCheck: September 3, 2024. Date of online publication: October 4, 2024.

This work was supported in part by the National Natural Science Foundation of China (No. 52377075) and Fundamental Research Funds for the Central Universities (No. 2024CDJXY006).

T. Niu, H. Li, G. Chen (corresponding author), S. Fang, and R. Liao are with the State Key Laboratory of Power Transmission Equipment & System Security and New Technology at Chongqing University, Chongqing 400044, China (e-mail: niutthu@qq. com; 892897009@qq. com; ghchen2023@cqu. edu. cn; fangston@cqu.edu.cn; rjliao@cqu.edu.cn).

DOI: 10.35833/MPCE.2024.000227

tablished a cooperative game-based scheduling strategy to maximize and allocate overall benefits. Reference [12] proposed a strategy based on the Shapley value theory to allocate benefits according to the contribution of each MG in the cooperative alliance. However, when faced with problems involving many MGs, the strategies based on Shapley value theory often suffer from issues such as long computation time and low solution quality. As an alternative approach, [13]-[16] established a cooperative game strategy for multiple MGs using the Nash bargaining game (NBG) model. This strategy maximizes the Nash product of the benefit of each MG as the objective function, and decomposes the problem into two subproblems: maximizing the benefit of coalition and evenly allocating the cooperative benefit. This strategy considers both individual interests and social benefits, aiming to achieve Pareto efficiency.

TABLE I
COMPARISON OF PRICING AND SCHEDULING STRATEGIES FOR MMGS

Reference	Pricing						Scheduling			
	Fixed price	SDR	Bidding	Marginal price	NBG		Game-based			Nongame-based: global optimization
					Symmetric NBG	Asymmetric NBG	Cooperative game		Noncooperative game: Stackelberg	
							NBG	Shapley		
[8]-[11]	√									√
[12]								√		
[13], [14]					√		√			
[15], [16]						√	√			
[17], [18]									√	
[19]		√								√
[20]		√							√	
[21], [22]			√							
[23]				√						√
This paper		√					√			

The noncooperative game strategy considers the leader−follower relationship between MGs and the main grid. A bilevel optimization model based on the Stackelberg game was adopted in [17], [18], where the upper-level main grid determines the time-of-use transaction prices, and the lower-level MGs determine the power exchange schedules with the main grid according to the prices. Through iterative modification of prices and power exchange schedules, a Stackelberg game equilibrium is achieved, where none of the MGs is willing to change its power exchange schedule any more. For the noncooperative game strategies, each MG operates independently to maximize its own benefit. The competitive relationship hinders collaboration among MGs, which usually leads to a loss of Pareto efficiency and social welfare optimality.

Determining collaborative prices is another crucial factor in the trading process among multiple MGs. References [8]-[11] set fixed prices, neglecting complex dynamics between prices and trading schedules. References [19] and [20] developed a pricing strategy considering supply−demand relationships, which reflects the commodity attributes of electricity and is computationally convenient in determining the electricity prices to motivate inter-transactions within MMGS. References [21] and [22] proposed a pricing strategy based on the auction mechanism, where MGs utilize smart contracts to conduct multiple rounds of bidding to ultimately achieve transaction matching. This strategy can fully leverage the advantages of blockchain networks, such as transparency in public information and tamper-proof transaction data. However, it relies heavily on smart meters to collect and evaluate fluctuations in market prices, rendering the overall process relatively complex. Reference [23] utilized the marginal pricing, which determines prices on the basis of the calculation of marginal cost increments with clear physical meanings. Nevertheless, in practical applications, marginal pricing is highly sensitive to the physical parameters and operating conditions of the power grid. Specifically, grid congestion significantly impacts electricity prices, leading to excessive price volatility risks for power generators and users. Game-based strategies are also widely used for price determination, especially those based on NBG model. It realizes benefit allocation by formulating P2P collaborative prices. In this process, [13] and [14] employ a symmetric pricing allocation strategy, which means that each MG receives a relatively equal allocation of benefits, regardless of the individual contribution of each MG. References [15] and [16] adopted the asymmetric NBG (A-NBG) model, which further quantifies the contribution of each entity during collaboration, and more benefits are distributed to entities with greater contribution proportions. However, in the strategies based on NBG/A-NBG model, trading plans are previously determined before prices, and prices only affect the actual benefits of MGs, but cannot affect trading schedules. Furthermore, it requires significant computational resources to handle larger system sizes and may encounter convergence difficulties.

The aforementioned studies focus mainly on MMGS pricing and scheduling strategies for the electricity market, where carbon emissions are considered a secondary aspect of electricity production. With the steady progress towards the goal of “carbon neutrality”, China has been promoting the carbon allowance market, where transaction mechanisms such as carbon allowance trading and tradable green certificate have gradually emerged to promote clean energy and reduce carbon emissions [24]. For the MMGS, there is a complex interdependence and a strong correlation between electricity generation and carbon emissions. Since the cost of trading carbon allowance is a crucial part of the total costs of MGs, MGs are forced to consider carbon allowance prices during the energy optimization scheduling, which in turn affects the electricity trading and the formulation of clearing prices. Ultimately, effective coordination between the electricity and carbon allowance markets promotes the goals of energy conservation and emission reduction. Reference [25] introduced the carbon allowance trading into the scheduling process while considering the impact of wind power uncertainty, and demonstrated the conduciveness of carbon allowance trading to reduce costs under the mandatory limitations of carbon emissions. Reference [26] further elaborated on the impact of the carbon allowance trading mechanism on the output of thermal power units.

The aforementioned studies provide significant theoretical discussions on the role of carbon allowance trading, but overlook the exploration of their synergistic effects with electricity trading mechanisms. As the direct target of policy implementation, more detailed analyses of both electricity and carbon allowance trading are required by dispatching systems to explore the effectiveness of coupled electricity−carbon market policy designs. Reference [27] explored the impact of carbon allowance trading policies on power generation planning in an integrated environment of the electricity market, carbon allowance market, and fuel market, enabling power generation companies to reasonably balance the relationship between emission reduction and profitability in a multi-interactive market context. However, this study focused more on the response of power generation companies to carbon emission policies. MGs typically include power sources and loads of both electric and thermal energy, so the impact of the coupled electricity−carbon market on the MMGS requires further investigation. In [28], a bilevel operational optimization model for the MMGS considering carbon allowance trading and demand response was established, which promotes the sharing of carbon allowance and electric energy, effectively reducing the total operation cost and total carbon emissions of the MMGS. Reference [29] further considered the trading processes of thermal energy and natural gas, and established a low-carbon economic dispatch model suitable for an integrated electricity–heat–gas supply system.

Through an investigation and analysis of existing research, studies on pricing of the coupled electricity−carbon market are still lacking. Among the current pricing strategies, transaction prices obtained through heuristic algorithms exhibit strong randomness and relatively ambiguous physical meanings. While prices derived from market principles and the bidding process have relatively clear physical implications, they rely on more accurate unit model information that is often difficult to obtain, and the calculation process is comparatively complex. In strategies based on the traditional NBG model, the dispatch schedule of the system is determined first, and then the collaborative prices are accordingly set, which fails to reflect the response process of individual MGs to price changes. The Stackelberg-based strategy can capture the interactive iteration between MGs and the upper-level market. However, owing to its nature as a noncooperative game, it cannot account for synergistic collaboration among MGs and has difficulty balancing a fair distribution of benefits. Additionally, as independently operating and self-governing entities, MGs usually adopt distributed strategies when making decisions about electricity and carbon allowance trading and operation scheduling. However, the increase of decision variables, especially integer variables, in the individual optimization model of MGs may render fast convergence ineffective.

In this paper, we propose a pricing and distributed scheduling framework for the MMGS oriented towards the coupled electricity−carbon market. First, a comprehensive operation model for a typical MG is established. Then, an innovative pricing strategy is established, which considers the supply−demand relationships of the coupled electricity−carbon market within the MMGS. Next, an NBG-based optimization strategy for MMGS is developed, and an accelerated PCB-ADMM-based algorithm is developed to solve the optimal trading and scheduling schemes. The collaborative prices, as well as the trading and scheduling schemes, are iteratively and adaptively updated until the results reach equilibrium. Finally, an elaborate numerical study demonstrates that the proposed framework can effectively enhance the willingness of MGs to participate in collaborative electricity−carbon market and achieve benefit allocation.

The main contributions of this paper are as follows:

1) A novel pricing strategy that considers the supply−demand relationships of the coupled electricity−carbon market within the MMGS is proposed. This strategy more accurately reflects the dynamic relationship between prices and supply−demand in the coupled electricity−carbon market during all periods, compensating for the shortcomings of NBG-based strategies.

2) Under the pricing strategy, an NBG-based optimization strategy of MMGS is established to further optimize electricity and carbon allowance trading, as well as operation scheduling of the MMGS. This strategy ensures the fairness of the benefits gained by each MG while also demonstrating the response process of the MG scheduling to changes in market prices, reflecting market dynamics and objective economic principles.

3) An accelerated PCB-ADMM algorithm is adopted to solve the fully distributed trading and scheduling problems of the MMGS. By adopting variable step size updating and a block coordinate descent (BCD) loop, the convergence can be better guaranteed, and the convergence speed can also be increased compared with that of the classical ADMM algorithm, particularly for problems involving integer variables in mathematical formulations.

II. Collaborative Operation Architecture of MMGS

The basic architecture of the MMGS studied in this paper is illustrated in Fig. 1. From the perspective of the physical network, all MGs of the MMGS are connected to a common upstream distribution network and a common natural gas network. The distribution lines function as entitative energy paths for MGs to deliver electric power from/to their counterparts or upstream distribution networks. From the perspective of a communication and control network (cyber network), each MG is governed and managed by a local microgrid controller (L-MGC), which plays a crucial role in determining and regulating: ① the power generation of controllable units within the MG, such as photovoltaic (PV) systems, wind turbines (WTs), gas turbines (GTs), and gas boilers (GBs); ② charging/discharging power of the energy storage system (ESS); ③ electricity and carbon allowance traded with neighboring MGs in the MMGS; and ④ electricity and carbon allowance traded with the upstream distribution network.

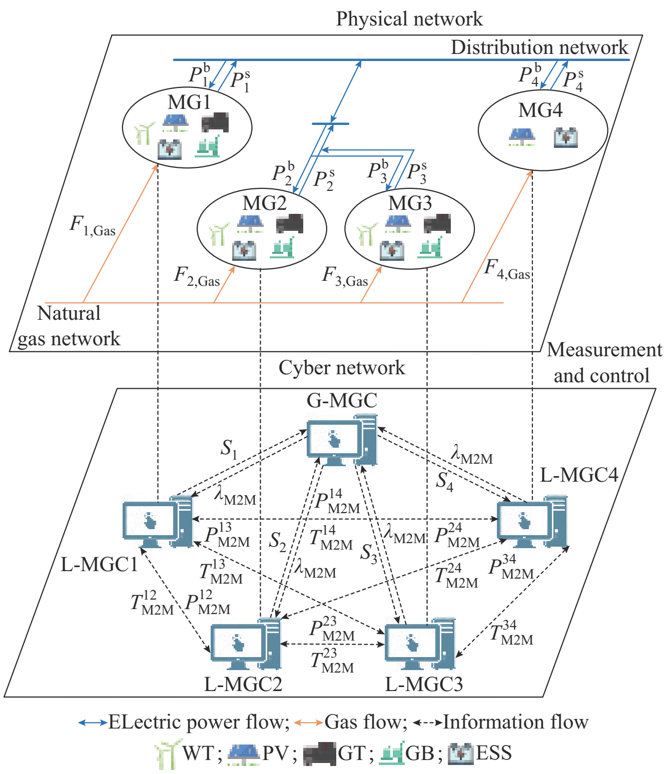

Fig. 1. Basic architecture of MMGS.

In addition to L-MGCs corresponding to every local MG, one global microgrid controller (G-MGC) governs the entire MMGS. As shown in Fig. 1, the L-MGC of each MG communicates with the G-MGC to exchange guidance information to achieve dynamic optimal operation. The G-MGC calculates the actual electric power/gas flow at the feeder/pipeline at the MG boundary and reports it to the distribution network operators (DNOs) and gas network operators (GNOs) as reference loads.

A. Exchange Process of System Energy

According to the external trading and internal scheduling instructions assigned by the L-MGC, the controllable units of each MG are regulated to the target value. At the macroscopic level, the electric power flows out from or into MGn are denoted by P_n^{s} and P_n^{b}, respectively, which comprise the electric power traded with the upstream distribution network and the electric power traded among MGn and its counterparts. Similar to the upstream distribution network, a common natural gas distribution network is also connected to each MG, and $F_{n,\mathrm{Gas}}$ represents the amount of natural gas purchased by MGn, which is used to supply the GT and GB.

B. Exchange Process of System Information

After completing the decision-making process, each L-MGC uploads its own electricity and carbon allowance trading results to the G-MGC through a private network. After trading schedules are gathered from all MGs, the G-MGC determines and updates the unified electricity price and carbon allowance price within the MMGS according to current supply–demand information and then broadcasts pricing signals to each L-MGC. All L-MGCs can also communicate with one another, enabling them to exchange electricity and carbon information and achieve P2P interactions. As shown in Fig. 1, $\boldsymbol{S}_n$ represents the decision results of the electricity and carbon allowance trading of MGn; λ_{M2M} represents the unified trading price broadcast from the G-MGC; P_{M2M}^{ij} represents the electricity traded between MGi and MGj; and T_{M2M}^{ij} represents the carbon allowance traded between MGi and MGj.

III. Collaborative Operation Model of MMGS

A. Energy Flow Model

Without loss of generality, we suppose that each investigated MG comprises one or more types of the aforementioned equipment, such as PV, WT, ESS, GT, or GB devices. Under this setting, it is possible to schedule conventional and renewable energy sources synergistically and to supply electric and thermal loads to energy consumers with greater flexibility.

1) Electric and Thermal Power Generation Units

1) The GT model is formulated as [30]:

$$P_{\mathrm{GT},t}=L_{\mathrm{GHV}}\eta_{\mathrm{GT}}F_{\mathrm{GT},t} \tag{1}$$

$$Q_{\mathrm{GT},t}=P_{\mathrm{GT},t}\eta_{\mathrm{r}}/\eta_{\mathrm{GT}} \tag{2}$$

$$0\leq P_{\mathrm{GT},t}\leq P_{\mathrm{GT,max}} \tag{3}$$

where $F_{\mathrm{GT},t}$ is the hourly usage of natural gas by the GT; $P_{\mathrm{GT},t}$ and $Q_{\mathrm{GT},t}$ are the electric and thermal power generated by the GT during period t, respectively; and $P_{\mathrm{GT,max}}$ is the upper limit of the electric power generation of the GT; L_{GHV} is the heating value of natural gas, which is typically taken as 9.7 kW·h/m^3; and η_{GT} and η_{r} are the electric power generation efficiency and heat recovery efficiency of the GT, respectively.

2) The GB model is formulated as:

$$Q_{\mathrm{GB},t}=L_{\mathrm{GHV}}\eta_{\mathrm{GB}}F_{\mathrm{GB},t} \tag{4}$$

$$0\leq Q_{\mathrm{GB},t}\leq Q_{\mathrm{GB,max}} \tag{5}$$

where $F_{\mathrm{GB},t}$ is the hourly usage of natural gas by the GB; $Q_{\mathrm{GB},t}$ is the thermal power generated by the GB during period t; η_{GB} is the thermal energy conversion efficiency of the GB; and $Q_{\mathrm{GB,max}}$ is the upper limit of the thermal power output of the GB.

2) ESS

The ESS model is formulated as:

$$S_{ES,t+1}=S_{ES,t}+(\eta_{cha}P_{cha,t}-P_{dis,t}\eta_{dis}^{-1}) \tag{6}$$

$$\begin{cases} 0\le P_{cha,t}\le U_{ES}P_{ES,max} \\ 0\le P_{dis,t}\le (1-U_{ES})P_{ES,max} \\ S_{ES,min}\le S_{ES,t}\le S_{ES,max} \end{cases} \tag{7}$$

where $S_{ES,t}$ is the initial electric energy of the ESS at the beginning of period t; η_{cha} and η_{dis} are the charging and discharging efficiencies of the ESS, respectively; $P_{cha,t}$ and $P_{dis,t}$ are the charging and discharging power of the ESS during period t, respectively; U_{ES} is a binary variable indicating the charging (1) or discharging (0) state of the ESS during period t; $P_{ES,max}$ is the maximum charging or discharging power of the ESS; and $S_{ES,min}$ and $S_{ES,max}$ are the lower and upper limits of the ESS capacity, respectively.

B. Carbon Allowance Trading Model

As an administrative measure to restrict carbon emission, a certain amount of free initial carbon allowance is allocated to power generation enterprises by government regulatory agencies, and excessive emissions are severely penalized. Moreover, power generation enterprises are allowed to purchase and sell carbon allowance through the carbon allowance market, which provides additional revenues and costs [28]. The carbon allowance trading model of MGs typically comprises three parts: an initial carbon allowance model, an actual carbon emission model, and a carbon allowance trading cost model.

1) The initial carbon allowance of each MG during period t is expressed as:

$$T_{CO_2,t}^{0}=\eta_{CO_2}^{RES}(P_{PV,t}+P_{WT,t})+\eta_{CO_2}^{GT}P_{GT,t}+\eta_{CO_2}^{GB}Q_{GB,t} \tag{8}$$

where $P_{PV,t}$ is the power generation of PV units during period t; $P_{WT,t}$ is the power generation of WT units; and $\eta_{CO_2}^{RES}$, $\eta_{CO_2}^{GT}$, and $\eta_{CO_2}^{GB}$ are the carbon allowance allocation coefficients of the renewable energy source (WT and PV), GT, and GB, respectively.

2) The actual carbon emission for an MG during period t is expressed as:

$$T_{CO_2,t}=\beta_{CO_2,GT}P_{GT,t}+\beta_{CO_2,GB}P_{GB,t} \tag{9}$$

where $\beta_{CO_2,GT}$ and $\beta_{CO_2,GB}$ are the carbon emission coefficients for the GT and GB, respectively.

3) The carbon allowance trading cost of an MG is expressed as:

$$C_{CO_2}=\sum_t(v_{M2G,t}^{b}T_{M2G,t}^{b}-v_{M2G,t}^{s}T_{M2G,t}^{s}+v_{M2M,t}T_{M2M,t}) \tag{10}$$

where $v_{M2G,t}^{b}$ and $v_{M2G,t}^{s}$ are the prices at which the carbon allowance is purchased from or sold to the upstream distribution network by each MG during period t, respectively; $v_{M2M,t}$ is the carbon allowance trading price with counterpart MGs; $T_{M2G,t}^{b}$ and $T_{M2G,t}^{s}$ are the carbon allowances purchased from and sold to the upstream distribution network by each MG, respectively; and $T_{M2M,t}=T_{M2M,t}^{b}-T_{M2M,t}^{s}$ is the total amount of carbon allowance traded with counterpart MGs, and a positive value indicates that the MG macroscopically purchases carbon allowance from other counterpart MGs.

C. Optimization Model for a Single MG

1) Objective Function

Each MG optimizes its internal controllable unit output and external electricity and carbon allowance trading schedule to minimize its total operation cost. Therefore, the objective function for each MG can be expressed as:

$$C_{MG}=C_{M2G}+C_{M2M}+C_{Gas}+C_{CO_2}+C_{OP}+C_{EM}-C_{SUB}-C_{DR} \tag{11}$$

$$\begin{cases} C_{M2G}=\sum_t(\lambda_{M2G,t}^{b}P_{M2G,t}^{b}-\lambda_{M2G,t}^{s}P_{M2G,t}^{s}) \\ C_{M2M}=\sum_t\lambda_{M2M,t}P_{M2M,t} \\ C_{Gas}=\sum_t\lambda_{Gas,t}(F_{GB,t}+F_{GT,t}) \\ C_{OP}=\sum_t\sum_m\lambda_m P_{m,t} \\ C_{EM}=\sum_t\sum_n\lambda_n P_{n,t} \\ C_{SUB}=\sum_t p_G(P_{PV,t}+P_{WT,t}) \\ C_{DR}=\sum_t p_{DR}(P_{DR,t}^{in}+P_{DR,t}^{de}) \end{cases} \tag{12}$$

where C_{MG} is the total operation cost of the MG; C_{M2G} is the payment for electricity trading with the upstream distribution network; $\lambda_{M2G,t}^{b}$ and $\lambda_{M2G,t}^{s}$ are the electricity prices for purchasing and selling electricity, respectively, which are assigned by the DNO; $P_{M2G,t}^{b}$ and $P_{M2G,t}^{s}$ are the electric power purchased from and sold to the upstream distribution network, respectively; C_{M2M} is the payment for electricity trading with counterpart MGs; $P_{M2M,t}=P_{M2M,t}^{b}-P_{M2M,t}^{s}$ is the total electric power traded with counterpart MGs, and $P_{M2M,t}^{b}$ and $P_{M2M,t}^{s}$ are the total electric power purchased from and sold to counterpart MGs during period t, respectively; $\lambda_{M2M,t}$ is the electricity price for interactive trading between MGs, which can be flexibly regulated by the G-MGC; C_{Gas} is the cost of natural gas procurement; $\lambda_{Gas,t}$ is the natural gas price; C_{OP} is the cost of equipment operation and maintenance; $P_{m,t}$ and λ_m are the output power and maintenance cost coefficient of device m (e.g., GT, GB, WT, PV, and ESS), respectively; C_{EM} is the environmental cost of gas emissions; λ_n is the environmental penalty cost coefficient for pollutant-emitting device n (e.g., GT and GB); $P_{n,t}$ is the corresponding output of pollutant-emitting device n; C_{SUB} is the subsidized revenue from renewable energy power generation; p_G is the subsidized price per unit of renewable energy power generation; C_{DR} is the subsidized revenue gained due to demand response participation; p_{DR} is the subsidized price per unit of electric power adjustment; and $P_{DR,t}^{in}$ and $P_{DR,t}^{de}$ are the power increase and decrease during period t due to demand response, respectively.

2) Constraints

To ensure the stability of MG operations, the following operational constraints must be satisfied.

1) Electric/thermal power balance constraints:

$$\begin{cases} P_{L,t}=P_{GT,t}+P_{ES,t}+P_{DR,t}+P_{PV,t}+P_{WT,t}+P_t^b-P_t^s \\ Q_{L,t}=Q_{GB,t}+Q_{GT,t} \end{cases} \tag{13}$$

where $P_{L,t}$ and $Q_{L,t}$ are the electric and thermal loads of the MG during period t, respectively; $P_{ES,t}$ is the power supplied by the ESS during period t; $P_{DR,t}=P_{DR,t}^{de}-P_{DR,t}^{in}$ is the load adjustment amount due to demand response participation; $P_t^b=P_{M2G,t}^b+P_{M2M,t}^b$ is the total purchased electric power of the MG during period t; and $P_t^s=P_{M2G,t}^s+P_{M2M,t}^s$ is the total sold electric power of the MG during period t.

2) Carbon allowance balance constraints:

$$T_{CO_2,t}^0+T_t^b=T_{CO_2,t}+T_t^s \tag{14}$$

where $T_t^b=T_{M2G,t}^b+T_{M2M,t}^b$ is the total carbon allowance of the MG bought from the upstream and carbon allowance markets during period t; and $T_t^s=T_{M2G,t}^s+T_{M2M,t}^s$ is the total carbon allowance of the MG sold to the upstream and carbon allowance markets during period t.

Unlike the strict real-time balance in the electricity market, the carbon allowance balance is often checked and cleared over a relatively long time horizon (such as one month or one year [29], depending on the carbon allowance market policy) in the current stage. Therefore, constraint (14) is actually stricter, necessitating the balance during each short time period and naturally ensuring balance over a long time horizon. To further explore the shifting flexibility of carbon allowance trading, carbon allowance trading can be scheduled on a longer time scale in future follow-up studies, i. e., medium- and long-term market before the day-ahead market in this work.

3) Electric power trading constraints:

$$\begin{cases} 0\le P_{*,t}^b\le U_{b,t}^{E,*}P_*^{b,\max} \\ 0\le P_{*,t}^s\le U_{s,t}^{E,*}P_*^{s,\max} \quad *=\{M2M, M2G\} \\ U_{b,t}^{E,*}+U_{s,t}^{E,*}\le 1 \end{cases} \tag{15}$$

where the superscript max represents the maximum value of corresponding variables; and $U_{b,t}^{E,*}$ and $U_{s,t}^{E,*}$ are the binary variables representing the state of power purchase or sale, respectively, which cannot be set to be 1 simultaneously.

4) Carbon allowance trading constraints:

$$\begin{cases} 0\le T_{*,t}^b\le U_{b,t}^{C,*}T_*^{b,\max} \\ 0\le T_{*,t}^s\le U_{s,t}^{C,*}T_*^{s,\max} \quad *=\{M2M, M2G\} \\ U_{b,t}^{C,*}+U_{s,t}^{C,*}\le 1 \end{cases} \tag{16}$$

where $U_{b,t}^{C,*}$ and $U_{s,t}^{C,*}$ are the binary variables representing the state of carbon allowance purchase or sale, respectively, which cannot be set to be 1 simultaneously.

5) Demand response constraints:

$$\begin{cases} 0\le P_{DR,t}^{in}\le U_{DR,t}^{in}\eta_{DR}^{in}P_{L,t} \\ 0\le P_{DR,t}^{de}\le U_{DR,t}^{de}\eta_{DR}^{de}P_{L,t} \\ U_{DR,t}^{in}+U_{DR,t}^{de}\le 1 \end{cases} \tag{17}$$

where η_{DR}^{in} and η_{DR}^{de} are the percentile ranges within which the load power can be adjusted; and $U_{DR,t}^{in}$ and $U_{DR,t}^{de}$ are the binary variables representing the state of load increase or decrease during the demand response, respectively. For the case where both $U_{DR,t}^{in}$ and $U_{DR,t}^{de}$ are 0, the MG does not participate in the demand response.

IV. Collaborative Pricing Models Within MMGS

As key factors dominating MMGS operation, electricity and carbon allowance prices greatly affect the collaborative scheduling and trading plans of the MMGS. This paper presents a pricing strategy that considers the supply−demand relationship, which is tractable to determine reasonable electricity and carbon allowance prices within the MMGS. Referring to [19], the collaborative pricing models can be obtained as follows.

A. Collaborative Electricity Pricing Model

After autonomous optimization, the power surplus/deficit of the MMGS during every time period can be evaluated, directly affecting collaborative electricity prices. To be more specific, we use P_t^{sup} to represent the total electricity supply of the MMGS during period t, which is calculated by adding up electricity sold of MGi at that time, i. e., $P_t^{sup}=\sum_i P_{i,t}^s$. And we use P_t^{de} to represent the total electricity demand of the MMGS during period t, which is the sum of the electricity purchased by MGi at that time, i.e., $P_t^{de}=\sum_i P_{i,t}^b$.

1) When $P_t^{sup}<P_t^{de}$, define the SDR of the electricity during period t by $\chi_t^E=P_t^{sup}/P_t^{de}$, and the collaborative electricity price is determined by:

$$\lambda_{M2M,t}=\frac{\lambda_{M2G,t}^b(\lambda_{M2G,t}^b+\lambda_{M2G,t}^s)}{\lambda_{M2G,t}^b(1+\chi_t^E)+\lambda_{M2G,t}^s(1-\chi_t^E)} \tag{18}$$

2) When $P_t^{sup}>P_t^{de}$, define the demand−supply ratio of the electricity during period t by $\delta_t^E=P_t^{de}/P_t^{sup}=1/\chi_t^E$, and the collaborative electricity price is determined by:

$$\lambda_{M2M,t}=\frac{\lambda_{M2G,t}^s(\lambda_{M2G,t}^b+\lambda_{M2G,t}^s)}{\lambda_{M2G,t}^s(1+\delta_t^E)+\lambda_{M2G,t}^b(1-\delta_t^E)} \tag{19}$$

3) When $P_t^{sup}=P_t^{de}\ne 0$, the collaborative electricity price is determined by:

$$\lambda_{M2M,t}=(\lambda_{M2G,t}^b+\lambda_{M2G,t}^s)/2 \tag{20}$$

This situation can be regarded as the boundary case, i.e., $\chi_t^E=1$, of the two cases above, where the clearing price keeps continuous over the entire definitional domain of $\chi_t^E>0$.

B. Collaborative Carbon Allowance Pricing Model

Similarly, we use T_t^{sup} to represent the total carbon allowance supply of the MMGS during period t, which is the sum of the carbon allowance sold by MGi at that time, i.e, $T_t^{sup}=\sum_i T_{i,t}^s$. And we use T_t^{de} to represent the total carbon allowance demand of the MMGS during period t, which is the sum of the carbon allowance purchased by MGi at that time, i.e., $T_t^{de}=\sum_i T_{i,t}^b$.

1) When $T_t^{sup}<T_t^{de}$, the collaborative carbon allowance price is determined by:

$$v_{M2M,t}=\frac{v_{M2G,t}^b(v_{M2G,t}^b+v_{M2G,t}^s)}{v_{M2G,t}^b(1+\chi_t^C)+v_{M2G,t}^s(1-\chi_t^C)} \tag{21}$$

where $\chi_t^C = T_t^{\text{sup}}/T_t^{\text{de}}$ is the SDR of carbon allowance during period t.

2) When $T_t^{\text{sup}} > T_t^{\text{de}}$, the collaborative carbon allowance price is determined by:

$$v_{\text{M2M},t} = \frac{v_{\text{M2G},t}^{\text{s}}\left(v_{\text{M2G},t}^{\text{b}} + v_{\text{M2G},t}^{\text{s}}\right)}{v_{\text{M2G},t}^{\text{s}}\left(1+\delta_t^C\right) + v_{\text{M2G},t}^{\text{b}}\left(1-\delta_t^C\right)} \tag{22}$$

where $\delta_t^C = T_t^{\text{de}}/T_t^{\text{sup}} = 1/\chi_t^C$ is the demand−supply ratio of carbon allowance during period t.

3) When $T_t^{\text{sup}} = T_t^{\text{de}} \neq 0$, the collaborative carbon allowance price is determined by:

$$v_{\text{M2M},t} = \left(v_{\text{M2G},t}^{\text{b}} + v_{\text{M2G},t}^{\text{s}}\right)/2 \tag{23}$$

C. Dynamic Mechanism Analysis of Price

Taking the collaborative electricity price as an example for analysis, the dynamic curve of market price as a function of SDR is shown in Fig. 2(a), where $\lambda_{\text{a}} = \left(\lambda_{\text{M2G},t}^{\text{b}} + \lambda_{\text{M2G},t}^{\text{s}}\right)/2$. The aforementioned collaborative electricity pricing model ensures that the collaborative electricity price curve is always located between the purchase and sale price levels of the upstream distribution network, enhancing the profitability of transaction participants and strengthening the willingness of various MGs to engage in collaboration. Similarly, the dynamic curve of collaborative carbon allowance price as a function of SDR follows the same pattern.

In addition, under the proposed pricing strategy, the collaborative electricity/carbon allowance price smoothly decreases as the SDR increases. The mechanism and reasonableness can be explained by analyzing the supply−demand relationship of the electricity/carbon allowance market during different periods. Still taking the electricity market for demonstration, Fig. 2(b) illustrates the demand curve (red solid curve D) and supply curve (blue solid curve S) with their intersection point E as the original market equilibrium point. Suppose that more output power can be generated during a certain period, which would result in the supply curve shifting to the right from S to S_1 (more supply quantity can be accessed for the same price). Thus, the market equilibrium point would change from point E to F, indicating a decrease in the market price during this period. Therefore, it can be deduced that the price tends to decrease with a higher SDR value, which aligns with Fig. 2(a). Similarly, with higher electric and thermal loads during peak-load periods, the demand curve shifts from D to D_1, and the market equilibrium point changes from point E to G, indicating an increase in the market price. This indicates that the price will be higher if a lower SDR value appears during some periods, as illustrated in Fig. 2(a).

V. NBG-based Optimization Strategy of MMGS and Distributed Solution Method

This section first establishes an NBG-based optimization strategy that is easy to solve in a distributed manner by referring to the collaborative prices. This strategy accounts for the balance of operation gains among the participant MGs in the MMGS. Subsequently, an improved accelerated PCB-ADMM algorithm is employed to solve the NBG-based optimization model.

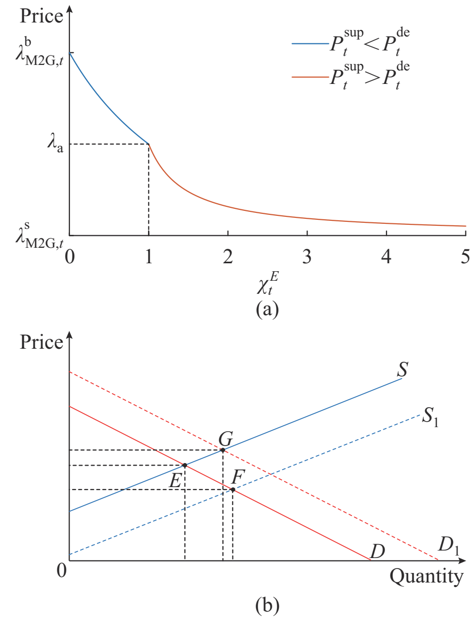

Fig. 2. Dynamic curves of market price. (a) Price curves related to SDR. (b) Price curves related to supply and demand variations.

A. NBG-based Optimization Strategy

As an independent entity in an MMGS, each MG is considered rational. Consequently, it is assumed that an MG will not engage in MMGS collaboration unless its operation revenue can be improved by collaboration. To achieve equilibrium of the complex game relationships among MGs, NBG model is adopted to develop the collaborative optimization of MMGS. In this work, we use the reduction in the operation cost of an MG after collaboration to represent the increase in operation revenue or benefit. Thus, the NBG model for collaborative optimization of MMGS can be formulated as follows:

$$\begin{cases} \max \prod_i \left(C_{\text{MG},i}^0 - C_{\text{MG},i}\right) \\ \text{s.t. } C_{\text{MG},i}^0 \geq C_{\text{MG},i} \\ \quad (1)\text{-}(11),\ (13)\text{-}(17) \end{cases} \tag{24}$$

where $C_{\text{MG},i}^0$ is the total operation cost of MGi before participating in collaboration; and $C_{\text{MG},i}$ is the operation cost of MGi after participating in collaboration.

Owing to the Pareto efficiency and convexity of the NBG problem, [31] demonstrated that an equilibrium solution for the NBG problem (24) exists and is unique, where the maximization of the Nash product of the increase in the revenue of all MGs is guaranteed. The proof indicates that in the NBG model, if the objective function is continuous over a bounded and compact feasible region of decision variables, a finite upper bound of the objective function must exist. As shown in (24), the decision variables of the NBG model refer to the power exchanged among MGs occurring within a finite range, and the continuous objective function is the product of the incremental revenue of the MG. Therefore, the conditions for the existence of a Nash bargaining solution are satisfied.

Since (24) is a nonconvex and nonlinear optimization problem, it is difficult to solve directly. The analysis reveals that the nonconvex and nonlinear nature of the problem stems from two aspects: the objective function of the Nash product and the binary variables in the constraints. For the problem of products in the objective function, since the natural logarithmic function is a monotonically increasing convex function, we take the negative logarithm of (24) to transform the original problem of maximizing the Nash product into minimizing the summation of a series of negative logarithmic functions (25).

$$\begin{cases} \min\left\{-\sum_i \ln(C^0_{\mathrm{MG},i}-C_{\mathrm{MG},i})\right\} \\ \text{s.t. } C^0_{\mathrm{MG},i} \geq C_{\mathrm{MG},i} \\ \quad (1)\text{-}(11),(13)\text{-}(17) \end{cases} \tag{25}$$

Owing to the coupling variables $P^{ij}_{\mathrm{M2M},t}$ and $T^{ij}_{\mathrm{M2M},t}$ in $C_{\mathrm{MG},i}$, which represent the electric power and carbon allowance traded between MGi and MGj, respectively, the consistency constraints in (26) should be met.

$$\begin{cases} P^{ij}_{\mathrm{M2M},t}+P^{ji}_{\mathrm{M2M},t}=0 \\ T^{ij}_{\mathrm{M2M},t}+T^{ji}_{\mathrm{M2M},t}=0 \end{cases} \tag{26}$$

B. Solution Method Based on Accelerated PCB-ADMM Algorithm

In this work, we adopt an improved accelerated PCB-ADMM algorithm [32] to solve the reformulated model (25) in a distributed manner, which can improve the convergence performance of ADMM algorithm and accelerate the convergence speed, especially for multi-block separable problems comprising various binary or integer variables.

For convenience of expression, we use N_i to represent the set of MGs connected to MGi, and $\left|N_i\right|$ represents the number of elements in set N_i. Based on (25), the augmented Lagrangian function for each MG is established as:

$$\begin{aligned} L_i = & -\ln(C^0_{\mathrm{MG},i}-C_{\mathrm{MG},i}) + \sum_{j\in N_i}\Big[(\boldsymbol{\psi}^{ij})^{\mathrm{T}}(\boldsymbol{P}^{ij}_{\mathrm{M2M}}+\boldsymbol{P}^{ji}_{\mathrm{M2M}})+ \\ & (\boldsymbol{\zeta}^{ij})^{\mathrm{T}}(\boldsymbol{T}^{ij}_{\mathrm{M2M}}+\boldsymbol{T}^{ji}_{\mathrm{M2M}})+\frac{\rho}{2}\left\|\boldsymbol{P}^{ij}_{\mathrm{M2M}}+\boldsymbol{P}^{ji}_{\mathrm{M2M}}\right\|_2^2+ \\ & \frac{\rho}{2}\left\|\boldsymbol{T}^{ij}_{\mathrm{M2M}}+\boldsymbol{T}^{ji}_{\mathrm{M2M}}\right\|_2^2\Big] \end{aligned} \tag{27}$$

where $\boldsymbol{P}^{ij}_{\mathrm{M2M}}=\bigcup_{t=1:T}P^{ij}_{\mathrm{M2M},t}$ and $\boldsymbol{T}^{ij}_{\mathrm{M2M}}=\bigcup_{t=1:T}T^{ij}_{\mathrm{M2M},t}$ are the vectors of power and carbon allowance purchased/sold by MGi from/to MGj during all periods, respectively; $\boldsymbol{P}^{ji}_{\mathrm{M2M}}=\bigcup_{t=1:T}P^{ji}_{\mathrm{M2M},t}$ and $\boldsymbol{T}^{ji}_{\mathrm{M2M}}=\bigcup_{t=1:T}T^{ji}_{\mathrm{M2M},t}$ are the vectors of corresponding consistent variables from the perspective of MGj; $\boldsymbol{\psi}^{ij}$ and $\boldsymbol{\zeta}^{ij}$ are the related Lagrange multiplier vectors concerning electricity and carbon allowance trading constraints (26) during all periods, respectively; and ρ is the penalty coefficient.

PCB-ADMM algorithm is a modified ADMM algorithm dedicated to multi-block separable convex optimization problems that implement distributed collaboration by sequentially carrying out two fundamental steps: prediction and correction. For the prediction step, a BCD loop is used, i.e., predicting each subproblem block in sequence following the order of $1\rightarrow 2\rightarrow \ldots \rightarrow n\rightarrow n-1\rightarrow \ldots \rightarrow 2$. For the correction step, a simple convex combination of two iteration points is computed from the prediction step and previous iteration. Owing to the block-separating and loop iteration procedure, the PCB-ADMM algorithm can accelerate the convergence speed more effectively than the traditional ADMM algorithm, especially for problems with multi-block separable convex optimization and integer variables [32]. The MMGS studied in this paper involves multiple MGs and therefore can be naturally regarded as a multi-block optimization problem. To further increase the convergence speed, this paper incorporates a dynamic penalty factor into the original PCB-ADMM algorithm. The procedure for solving the cooperative operation model of the MMGS based on the accelerated PCB-ADMM algorithm is shown in Algorithm 1, where ρ_0 is the initial value of the penalty factor, which is set to be 10^{-6}; τ is the adjustment factor, which is set to be 0.15; α is the correction step size, which is set to be 0.95; and γ is the iteration residual.

Algorithm 1: accelerated PCB-ADMM algorithm

Set iteration counter $k=0$

Initialization For MGi and MGj ($i,j\in N_i$), set initial values, including: ① Lagrange multipliers $\boldsymbol{\psi}^{ij}(0)$, $\boldsymbol{\zeta}^{ij}(0)$; ② coupling variables $\boldsymbol{P}^{ij}_{\mathrm{M2M}}(0)$, $\boldsymbol{T}^{ij}_{\mathrm{M2M}}(0)$; and ③ penalty coefficient $\rho(0)$

Do:

Prediction For MGi, use $\tilde{\boldsymbol{P}}^{ij}_{\mathrm{M2M}}(k)$ and $\tilde{\boldsymbol{T}}^{ij}_{\mathrm{M2M}}(k)$ to backup current values of coupling variables

Forward prediction: for $j=1,2,\ldots,\left|N_i\right|$,

fix $\boldsymbol{\psi}^{mi}(k),\boldsymbol{\zeta}^{mi}(k),\boldsymbol{P}^{mi}_{\mathrm{M2M}}(k),\boldsymbol{T}^{mi}_{\mathrm{M2M}}(k)\quad m\in\left[1{:}\left|N_i\right|\right]\backslash\{j\}$

update $[\boldsymbol{P}^{ij}_{\mathrm{M2M}}(k);\boldsymbol{T}^{ij}_{\mathrm{M2M}}(k)]\leftarrow\arg\min L_i(\boldsymbol{P}^{ij}_{\mathrm{M2M}};\boldsymbol{T}^{ij}_{\mathrm{M2M}})$

Backward prediction: for $j=\left|N_i\right|,\left|N_i\right|-1,\ldots,2$,

fix $\boldsymbol{\psi}^{mi}(k),\boldsymbol{\zeta}^{mi}(k),\boldsymbol{P}^{mi}_{\mathrm{M2M}}(k),\boldsymbol{T}^{mi}_{\mathrm{M2M}}(k)\quad m\in\left[2{:}\left|N_i\right|\right]\backslash\{j\}$

update $[\boldsymbol{P}^{ij}_{\mathrm{M2M}}(k);\boldsymbol{T}^{ij}_{\mathrm{M2M}}(k)]\leftarrow\arg\min L_i(\boldsymbol{P}^{ij}_{\mathrm{M2M}};\boldsymbol{T}^{ij}_{\mathrm{M2M}})$

Communication For MGi and MGj ($i,j\in N_i$), share local prediction values of coupling variables: $\boldsymbol{P}^{ij}_{\mathrm{M2M}}(k),\boldsymbol{P}^{ji}_{\mathrm{M2M}}(k),\boldsymbol{T}^{ij}_{\mathrm{M2M}}(k),\boldsymbol{T}^{ji}_{\mathrm{M2M}}(k)$

Correction For MGi and $j=1,2,\ldots,\left|N_i\right|$,

$\boldsymbol{\psi}^{ij}(k+1)=\boldsymbol{\psi}^{ij}(k)+\alpha\rho(k)(\boldsymbol{P}^{ij}_{\mathrm{M2M}}(k)+\boldsymbol{P}^{ji}_{\mathrm{M2M}}(k))$

$\boldsymbol{\zeta}^{ij}(k+1)=\boldsymbol{\zeta}^{ij}(k)+\alpha\rho(k)(\boldsymbol{T}^{ij}_{\mathrm{M2M}}(k)+\boldsymbol{T}^{ji}_{\mathrm{M2M}}(k))$

$\boldsymbol{P}^{ij}_{\mathrm{M2M}}(k+1)=\boldsymbol{P}^{ij}_{\mathrm{M2M}}(k)-\alpha(\tilde{\boldsymbol{P}}^{ij}_{\mathrm{M2M}}(k)-\boldsymbol{P}^{ij}_{\mathrm{M2M}}(k))$

$\boldsymbol{T}^{ij}_{\mathrm{M2M}}(k+1)=\boldsymbol{T}^{ij}_{\mathrm{M2M}}(k)-\alpha(\tilde{\boldsymbol{T}}^{ij}_{\mathrm{M2M}}(k)-\boldsymbol{T}^{ij}_{\mathrm{M2M}}(k))$

$\rho(k+1)=\rho_0\mathrm{e}^{k\tau}$

Communication For each MGi and MGj ($i,j\in N_i$), share corrected coupling variables and multipliers: $\boldsymbol{P}^{ij}_{\mathrm{M2M}}(k+1)$, $\boldsymbol{P}^{ji}_{\mathrm{M2M}}(k+1)$, $\boldsymbol{T}^{ij}_{\mathrm{M2M}}(k+1)$, $\boldsymbol{T}^{ji}_{\mathrm{M2M}}(k+1)$, $\boldsymbol{\psi}^{ij}(k+1)$, $\boldsymbol{\zeta}^{ij}(k+1)$

Accumulate iteration counter: $k\leftarrow k+1$

Until:

$\gamma=\left\|\boldsymbol{P}^{ij}_{\mathrm{M2M}}(k+1)+\boldsymbol{P}^{ji}_{\mathrm{M2M}}(k+1)\right\|_2^2+\left\|\boldsymbol{T}^{ij}_{\mathrm{M2M}}(k+1)+\boldsymbol{T}^{ji}_{\mathrm{M2M}}(k+1)\right\|_2^2\leq 10^{-2}$

C. Overall Solution Process

In summary, the overall solution process for pricing and distributed scheduling of the MMGS is described as follows.

Step 1: the G-MGC decides and broadcasts collaborative electricity price $\lambda_{\mathrm{M2M},t}$ and collaborative carbon allowance price $v_{\mathrm{M2M},t}$ to all L-MGCs. Then, L-MGCs perform iterative decisions based on accelerated PCB-ADMM algorithm according to these prices, until the iteration residual γ is less than the preset threshold 10^{-2}.

Step 2: each L-MGC transmits its final trading decisions to the G-MGC, according to which the G-MGC assesses SDRs in both the electricity and carbon allowance markets during each period.

Step 3: the G-MGC updates the electricity and carbon allowance prices following (18)-(23) and broadcasts them to L-MGCs as in *Step 1*.

Step 4: L-MGCs initiate a new round of distributed scheduling according to the latest trading prices, as in *Step 2*.

The overall solution process is iteratively conducted until the variances of electricity and carbon allowance prices are less than the preset threshold 10^{-4}.

VI. Case Study

A. System Parameters and Operation Framework Settings

The MMGS illustrated in Fig. 1 is used in this paper, which comprises 4 independent MGs. MG1, MG2, and MG3 are integrated energy systems that include WT, PV, ESS, and GT, whose parameters are adopted from [30]. MG4 is a solar energy storage plant that consists of PV and ESS. The investigated scheduling period is set to be 24 hours and is equally divided into 24 intervals. The power generation of PV and WT and load curves for each MG are shown in the Appendix A. The electricity purchase and sale prices of upstream distribution network are shown in the Appendix A Table AI. The carbon allowance purchase and sale prices of upstream distribution network are 0.025 and 0.05 ¥/kg, respectively.

To validate the effectiveness and rationality of the proposed strategies, comparative analyses are conducted on 4 different operation frameworks of the MMGS.

Framework 1: no P2P electricity and carbon allowance trading exists within the MMGS. Each MG can participate in electricity–carbon trading only with the upstream distribution network.

Framework 2: P2P electricity trading exists within the MMGS, but P2P carbon allowance trading is not available.

Framework 3: P2P electricity and carbon allowance trading exist within the MMGS. The NBG model in [14] is adopted for both pricing and scheduling.

Framework 4: P2P electricity and carbon allowance trading exist within the MMGS. The proposed SDR-based pricing and NBG-based optimization strategies are adopted.

B. Analysis of Convergence Performance

The results of the iterative convergence process are shown in Fig. 3.

The curves labeled 1-24 in Fig. 3(a) and Fig. 3(b) represent the price iteration curves for each time period. It can be found that both the electricity and carbon allowance prices tend to stabilize after 5 iterations. Moreover, comparisons of iteration residuals γ among ADMM algorithm, PCB-ADMM algorithm, accelerated ADMM algorithm with variable step sizes (denoted as algorithm A), and accelerated PCB-ADMM algorithm with variable step sizes (denoted as algorithm B) are shown in Fig. 3(d). The ADMM and PCB-ADMM algorithms with fixed penalty factors require 110 iterations and 107 iterations, respectively, for the dual residual to achieve convergence. However, the number of iterations under algorithms A and B are reduced to 64 and 42, respectively.

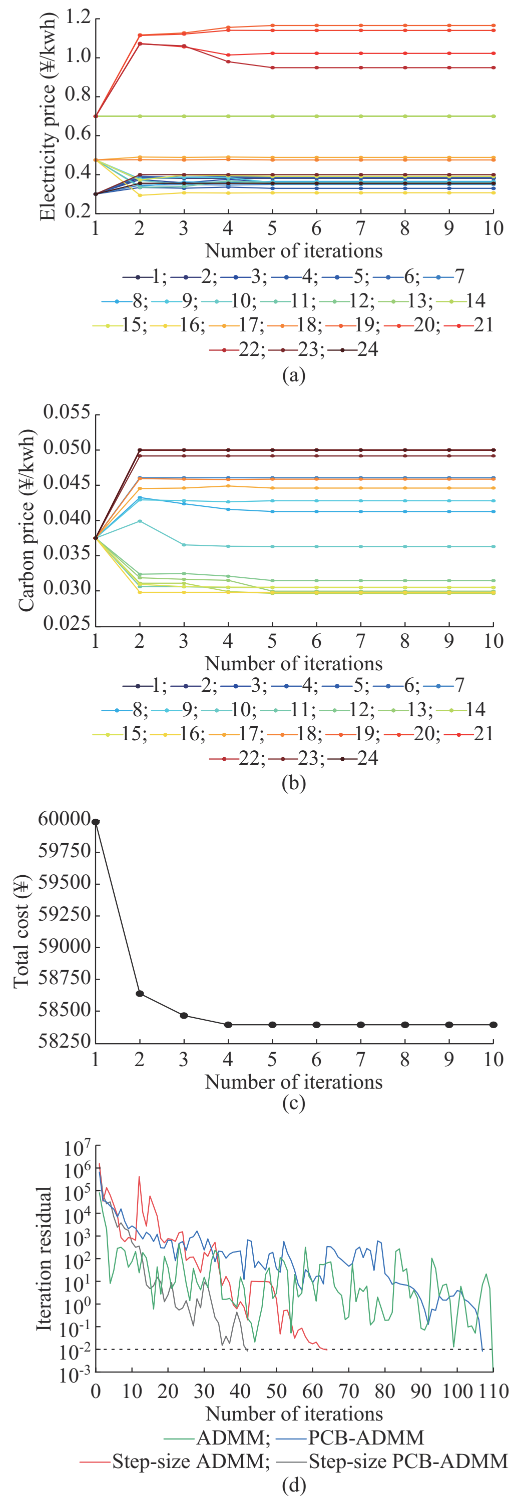

Fig. 3. Results of iterative convergence process. (a) Electricity price. (b) Carbon allowance price. (c) Total cost. (d) Iteration residuals under different algorithms.

The results indicate that the accelerated PCB-ADMM algorithm adopted in this work performs better with sufficient accuracy and rapid convergence.

C. Analysis of Pricing and Distributed Scheduling Results

1) Results of Collaborative Optimization

By solving the Framework 4, the transaction results of each MG are obtained and shown in Fig. 4. The following conclusions can be drawn from the transaction results.

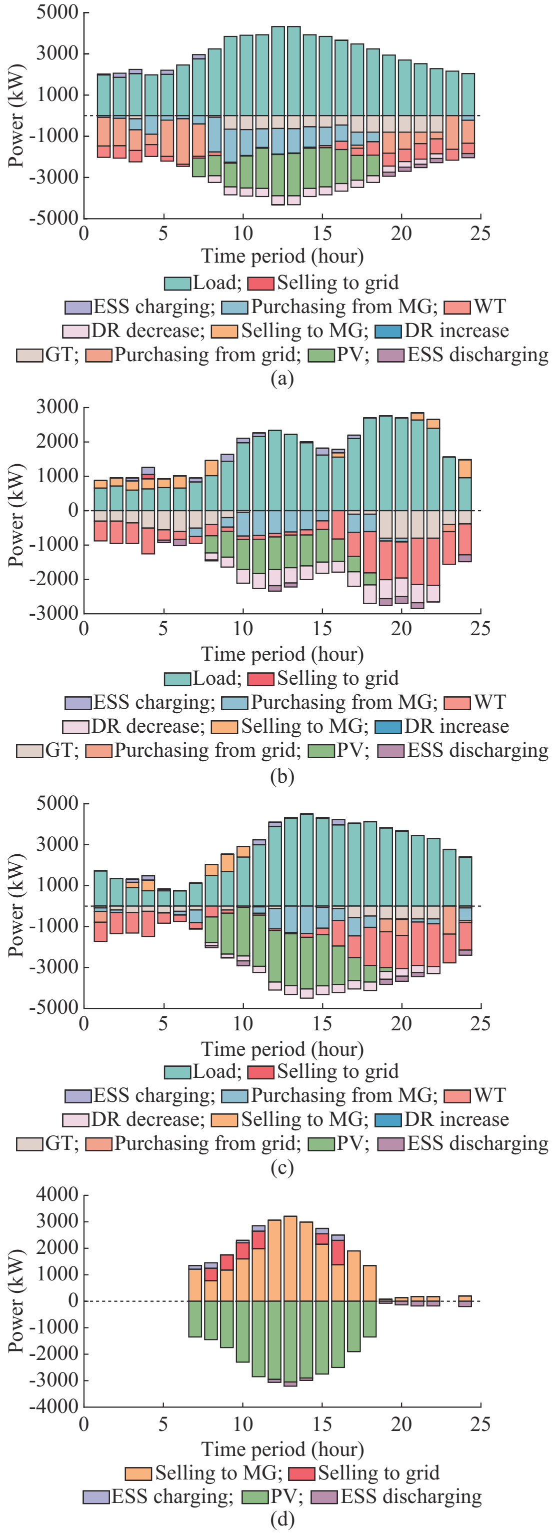

Fig. 4. Transaction results of each MG under collaborative optimization. (a) MG1. (b) MG2. (c) MG3. (d) MG4.

1) Each MG can maintain power balance during every period. Owing to the higher procurement cost of natural gas, high-cost GTs operate during periods of high electricity demand when the purchase price is higher, such as during periods of 9-22 hours for MG1. Additionally, the generation of renewable energy sources provides free carbon allowance. Therefore, in cases where there is a greater contribution from renewable energy sources, selling the electricity generated by the GT can generate additional revenue, as observed during periods of 23-24 hours and 1-8 hours for MG2.

2) In the case of a power deficit, each MG is designed to prioritize the fulfillment of the requisite electricity through P2P trading within the MMGS. Only when the electricity supply is unable to meet the electricity demand, MGs resort to purchasing electricity from the upstream distribution network. For instance, MG1 purchases a total of 1545.54 kW of electricity from the upstream distribution network.

3) Each MG has the ability to store a proportion of its energy through energy storage devices during periods of surplus generation or low electricity prices. The stored energy can then be used during periods of insufficient renewable energy power generation or high electricity prices. For example, MG1 has an average energy storage power of 120.3 kW during periods of 1-7 hours and an average energy discharge power of 160 kW during periods of 19-24 hours.

4) Additionally, each MG can actively respond to peak shaving requirement of the upstream distribution network by reducing its load during high-demand periods to receive certain subsidy revenues. For example, MG1 reduces its load by an average of 347.52 kW during the high-demand periods of 8-22 hours.

2) Trading Results of Carbon Allowance Market

The trading results of carbon allowance market is shown in Fig. 5. According to the results shown in Fig. 5(a), MG1 is the main carbon allowance buyer, with an average purchase of 65.33 kg of carbon allowance during each period. MG4 is the main carbon allowance seller, with an average sale of 80.14 kg of carbon allowance during each period. MG3 has higher renewable energy power generation during periods of 10-16 hours and lower GT power generation, resulting in greater carbon emission allowance sales during these periods, with an average value of 46.37 kg.

As for total carbon emission and total carbon emission costs of MMGS, when P2P carbon allowance trading is unavailable (Framework 2), each MG reduces its GT power generation by exchanging electricity among MGs, reducing the total carbon emission by 1.39%. In Frameworks 3 and 4, the coupled electricity–carbon market among MGs is considered, which encourages MGs to retain carbon allowance for trading to obtain more benefits. Therefore, the total carbon emissions under Frameworks 3 and 4 decrease by 5.95% and 4.88%, respectively. Figure 5(a) shows that MGs with high carbon emissions purchase carbon allowance from other MGs with surplus carbon allowance, thereby reducing the cost. Therefore, after considering P2P carbon allowance trading in Frameworks 3 and 4, the total carbon emission costs are reduced by 32.47% and 31.88%, respectively.

3) Results of Electricity and Carbon Allowance Prices

In Framework 4, the clearing electricity prices and carbon allowance prices among multiple MGs are characterized via the collaborative pricing model in Section IV. The calculation results of electricity price curve and carbon allowance price curve are shown in Fig. 6.

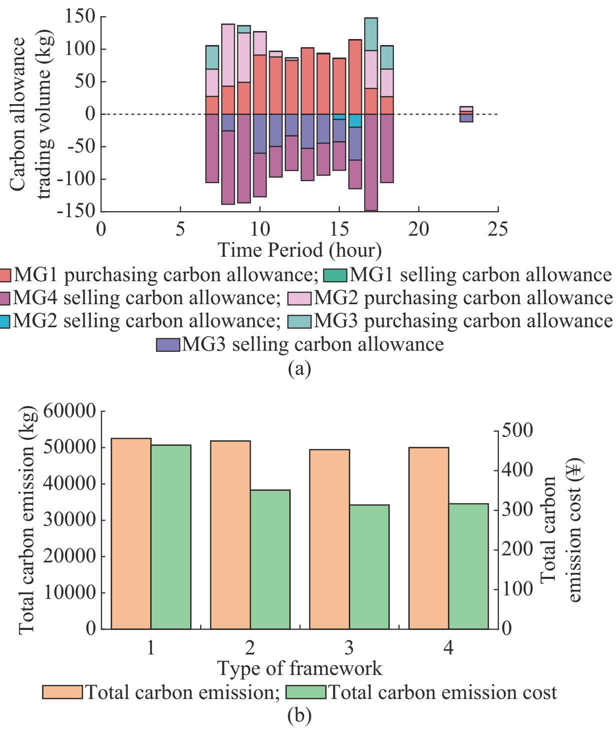

Fig. 5. Trading results of carbon allowance market. (a) Carbon allowance trading results under Framework 4. (b) Total carbon emission and total carbon emission cost results under Frameworks 1-4.

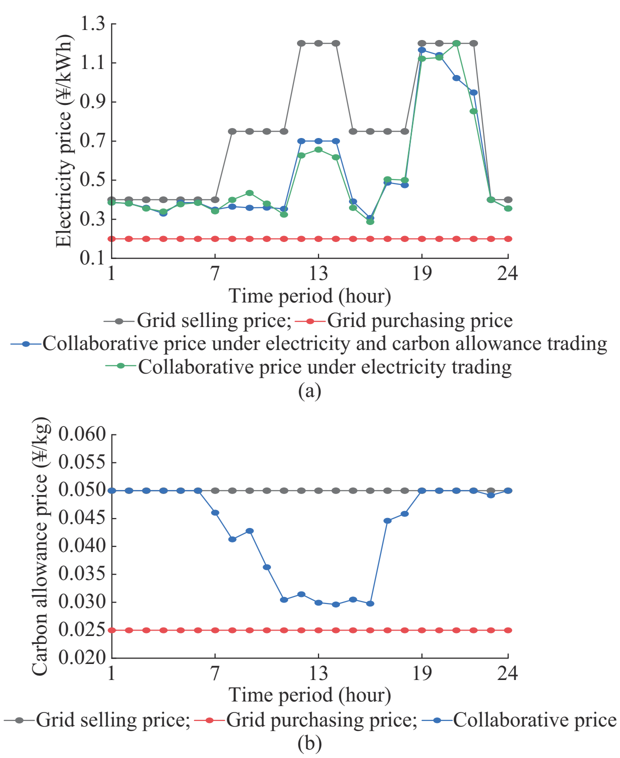

Fig. 6. Calculation results of electricity and carbon allowance prices during each trading period. (a) Electricity price. (b) Carbon allowance price.

In Fig. 6(a), the collaborative electricity prices during most periods are close to the selling prices of the upstream distribution network. This is due to the fact that the MMGS experiences supply–demand imbalance during nonpeak electricity consumption periods. For example, during periods of 23-24 hours and 1-7 hours, the average collaborative electricity price is 0.37 ¥/kWh. However, during the peak electricity consumption period, the solar energy storage plant in MG4 provides a large amount of electricity, resulting in collaborative electricity prices lower than the selling prices of the upstream distribution network, with an average reduction of 0.4 ¥/kWh. In operation frameworks without P2P carbon allowance trading (Frameworks 1 and 2), the carbon allowance of different MGs can be traded only with the upstream distribution network. The results show that during high electricity price periods of 12-15 hours and 19-22 hours, the total output of thermal power units without P2P carbon allowance trading increases by 728.86 kW on average. This indicates that the MG tends to utilize surplus carbon allowance for power generation when the collaborative price is high, in order to sell more electricity and generate more revenues, thus leading to an increase in electricity sales and a corresponding decrease in electricity prices. However, during the low electricity price periods of 7-10 hours, renewable energy power generation is lower, and the initial carbon allowance of the MG is limited, with an average decrease of 14.5% compared with that of the peak electricity consumption period, and the total electricity sales without considering P2P carbon allowance trading exhibit an average decline of 182.9 kW compared with that considering P2P carbon allowance trading. This indicates that when carbon allowance is insufficient, the MG selects to prioritize meeting its own electricity demand, which results in a reduction in electricity sales and a corresponding increase in electricity prices. It can be concluded that considering P2P carbon allowance trading process during the operation of the MMGS has an impact on the operational strategies of the MG.

Figures 5(a) and 6(b) show that during periods of 1-6 hours and 19-24 hours, all the MGs act as carbon allowance buyers. Therefore, the collaborative carbon allowance prices during these periods attain the carbon allowance selling price of the upstream distribution network, which is 0.05 ¥/kg. However, with the activation of the PV units, MG3 and MG4 are allocated with a substantial carbon allowance, which results in an increase in the carbon allowance supply in the carbon allowance market and a corresponding decrease in the collaborative carbon allowance price, which drops to 0.0302 ¥/kg.

D. Comparative Analysis Under Different Operation Frameworks of MMGS

The costs of individual MGs and the total costs of the MMGS under different operation frameworks are shown in Table II.

TABLE II
COST COMPARISON UNDER DIFFERENT OPERATION FRAMEWORKS

Framework	Cost (¥)				Total cost (¥)
	MG1	MG2	MG3	MG4	
1	38854.1	20514.5	18654.5	–6596.8	71426.3
2	36250.8	20310.9	18139.6	–9999.2	64702.1
3	34651.2	17511.6	15651.6	–10399.0	57414.8
4	34869.9	20118.6	17672.2	–14268.0	58392.4

In Framework 1, where there is no collaboration among MGs, the deficit and surplus electricity of each MG can be balanced only through transactions with the upstream distribution network, resulting in the worst economic performance. Compared with those of Framework 2, the costs of each MG in Frameworks 3 and 4 are significantly lower. This indicates that the framework considering P2P electricity and carbon allowance trading inspires collaboration and reduces the costs of MGs, greatly enhancing economic performance. Framework 3 achieves a relatively equitable distribution of revenue by traditional NBG model to determine both trading prices and schedules. Compared with the case of independent operation, Framework 3 yields even a relatively increase in revenue for each MG, with an increase of approximately ¥3502.9. However, due to the shortcoming of traditional NBG-based pricing strategies adopted in previous works, the actual market principle between prices and market supply−demand levels cannot be reflected. Although the results in Framework 3 achieve idealized revenue allocation, it is difficult to reflect the situation where the trading plans of MGs change with market prices in the actual market trading process. Framework 4 more accurately reflects the dynamic relationship between the scheduling strategy and the market price. By comparing Fig. 4 and Fig. 6, it can be observed that the MMGS is in a state of short supply for the majority of the trading process, particularly during the peak electricity consumption periods of 11-14 hours. Therefore, the income of the primary power supplier MG4 increases by ¥4169 compared with that of Framework 3, whereas the costs of MG1, MG2, and MG3, as demanders, increase by ¥518.7, ¥2607, and ¥2020.6, respectively, which more accurately reflects the rationality of actual market. Additionally, the total cost under Framework 4 increases by only ¥977.6 (1.7% in percentage) compared with that under Framework 3, indicating that the overall benefit under Framework 4 deviates little from the optimal benefit obtained under Framework 3.

E. Influence Analysis Under Interaction with an Upstream Distribution Network

To explore the influence of operation scheduling and collaborative willingness of the MMGS when it responds to the demand response adjustment of the upstream distribution network, a comparative analysis is conducted on the costs obtained under a demand response adjustment margin of 10% (i.e., the situation investigated in aforementioned results) and those obtained under a demand response adjustment margin of 20%. The results are presented in Table III.

TABLE III
COST COMPARISON UNDER DIFFERENT ADJUSTMENT MARGINS

Adjustment margin (%)	Cost (¥)				Total cost (¥)
	MG1	MG2	MG3	MG4	
10	34869.9	20118.6	17672.2	–14268.0	58392.4
20	30403.6	17146.1	14038.9	–11992.6	49596.1

As shown in Table III, the total cost decreases by ¥8796.3 when the adjustment margin increases from 10% to 20%, indicating that increasing the participation in demand response interactions with the upstream distribution network can increase the total profitability of the MMGS.

Among all the MGs, the main beneficiaries are MG1, MG2, and MG3, which earn extra benefits from demand response subsidies by further reducing their load demand. However, the load demand reduction also increases the SDR and decreases the collaborative electricity price. Consequently, a lower collaborative electricity price results in a further decrease in the benefit for the primary power supplier MG, such as MG4 in this study. This reveals an implicit risk that although the supplier MG is not directly involved in demand response, it may suffer from benefit loss due to price fluctuations. In this case, the overall demand response benefits must be reallocated to ensure that the benefits of the supplier MG are not affected.

VII. CONCLUSION

Taking coupled electricity−carbon market within MMGS into full consideration, this study focuses on operation optimization of multiple MGs with diverse stakeholders. A holistic operational framework, which comprises the SDR-based pricing strategy and the NBG-based optimization strategy, is constructed to promote collaborative electricity and carbon allowance trading within the MMGS, which effectively increases the economic and environmental revenue. The effectiveness and rationality of the proposed framework are verified and analyzed through case studies.

The framework proposed in this paper holds practical significance for realizing trading in the coupled electricity–carbon market of the MMGS. In future research, the impacts of power generation uncertainty on renewable energy and trading strategies under power flow constraints will be considered. The issue of how MMGS can more effectively interact with upstream distribution networks, especially during periods of peak demand or grid instability, is also a topic that warrants further in-depth exploration.

APPENDIX A

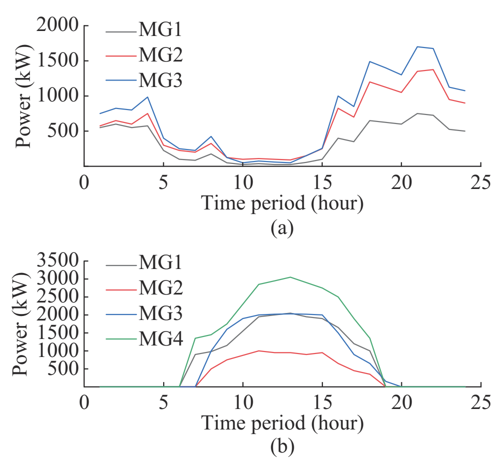

Fig. A1. Renewable energy power generation curves of each MG. (a) WT power generation. (b) PV power generation.

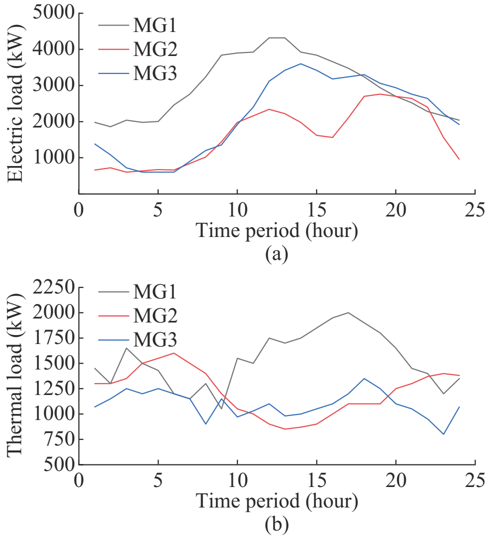

Fig. A2. Load curves of each MG. (a) Electric load. (b) Thermal load.

TABLE AI
ELECTRICITY PURCHASE AND SALE PRICES OF DISTRIBUTION NETWORK

Time period (hour)	Sale price (¥/kWh)	Purchase price (¥/kWh)
12-14, 19-22	0.2	1.20
8-11, 15-18	0.2	0.75
23-24, 0-7	0.2	0.40

REFERENCES

[1] Z. Zhang and C. Kang, "Challenges and prospects for constructing the new-type power system towards a carbon neutrality future," *Proceedings of the CSEE*, vol. 42, no. 8, pp. 2806-2819, Apr. 2022.

[2] B. Xin, B. Shan, Q. Li *et al.*, "Rethinking of the 'three elements of energy' toward carbon peak and carbon neutrality," *Proceedings of the CSEE*, vol. 42, no. 9, pp. 3117-3126, May 2022.

[3] E. Bullich-Massagué, F. Díaz-González, M. Aragüés-Peñalba *et al.*, "Microgrid clustering architectures," *Applied Energy*, vol. 212, pp. 340-361, Feb. 2018.

[4] K. Jithin, P. P. Haridev, N. Mayadevi *et al.*, "A review on challenges in DC microgrid planning and implementation," *Journal of Modern Power Systems and Clean Energy*, vol. 11, no. 5, pp. 1375-1395, Sept. 2023.

[5] L. Che, M. Khodayar, and M. Shahidehpour, "Only connect: microgrids for distribution system restoration," *IEEE Power and Energy Magazine*, vol. 12, no. 1, pp. 70-81, Jan. 2014.

[6] Y. Liu, X. Chen, B. Li *et al.*, "State of art of the key technologies of multiple microgrids system," *Power System Technology*, vol. 44, no. 10, pp. 3804-3820, Feb. 2020.

[7] W. Zhong, S. Xie, K. Xie *et al.*, "Cooperative P2P energy trading in active distribution networks: an MILP-based Nash bargaining solution," *IEEE Transactions on Smart Grid*, vol. 12, no. 2, pp. 1264-1276, Mar. 2021.

[8] S. Lin, C. Liu, D. Li *et al.*, "Bi-level multiple scenarios collaborative optimization configuration of CCHP regional multi-microgrid system considering power interaction among microgrids," *Proceedings of the CSEE*, vol. 40, no. 5, pp. 1409-1421, Dec. 2020.

[9] S. Ge, X. Chen, H. Liu *et al.*, "Market design of P2P electricity carbon coupling transaction among multi-microgrids in the zone," *High Voltage Engineering*, vol. 49, no. 4, pp. 1341-1349, Oct. 2023.

[10] C. Wang and N. Liu, "Distributed optimal dispatching of interconnected microgrid system based on alternating direction method of multipliers," *Power System Technology*, vol. 40, no. 9, pp. 2675-2681, Jul. 2016.

[11] H. Wang, Q. Ai, J. Wu *et al.*, "Bi-level distributed optimization for microgrid clusters based on alternating direction method of multipliers," *Power System Technology*, vol. 42, no. 6, pp. 1718-1727, Apr. 2018.

[12] R. Hu, Z. Wei, Y. Huang *et al.*, "Multi-microgrid joint economic dispatch based on alternating multiplier method and Shapley distribution method," *Electric Power Construction*, vol. 42, no. 7, pp. 28-38, Jul. 2021.

[13] X. Gu, Q. Wang, Y. Hu *et al.*, "Distributed low-carbon optimal operation strategy of multi-microgrids integrated energy system based on Nash bargaining," *Power System Technology*, vol. 46, no. 4, pp. 1464-1482, Mar. 2022.

[14] H. Wang and J. Huang, "Incentivizing energy trading for interconnected microgrids," *IEEE Transactions on Smart Grid*, vol. 9, no. 4, pp. 2647-2657, Jul. 2018.

[15] J. Wu, P. Lou, M. Guan *et al.*, "Operation optimization strategy of multi-microgrids energy sharing based on asymmetric Nash bargaining," *Power System Technology*, vol. 46, no. 7, pp. 2711-2723, Dec. 2022.

[16] H. Kim, J. Lee, S. Bahrami *et al.*, "Direct energy trading of microgrids in distribution energy market," *IEEE Transactions on Power Systems*, vol. 35, no. 1, pp. 639-651, Jan. 2020.

[17] X. You, H. Li, Y. Lu *et al.*, "Pricing strategy for multi-microgrid centralized trading considering distribution network power flow," *Power System Technology*, vol. 46, no. 4, pp. 1297-1309, May 2022.

[18] X. Li, R. Ma, and Y. Luo, "Price-based demand response of microgrid and optimal pricing strategy based on Stackelberg game," *Power System Protection and Control*, vol. 45, no. 5, pp. 88-95, Mar. 2017.

[19] N. Liu, X. Yu, C. Wang *et al.*, "Energy-sharing model with price-based demand response for microgrids of peer-to-peer prosumers," *IEEE Transactions on Power Systems*, vol. 32, no. 5, pp. 3569-3583, Sept. 2017.

[20] H. He, X. Lei, T. Huang *et al.*, "Coordinated and autonomous optimal operation strategy of multi-microgrid system under the guidance of price," *Power System Protection and Control*, vol. 47, no. 16, pp. 17-26, Aug. 2019.

[21] T. Chen, Y. Liu, W. Liu *et al.*, "Adaptive microgrid price-making strategy and economic dispatching method based on blockchain technology," *Electric Power Construction*, vol. 42, no. 6, pp. 17-28, Jun. 2021.

[22] J. Wang, N. Zhou, Q. Wang *et al.*, "Electricity direct transaction mode and strategy in microgrid based on blockchain and continuous double auction mechanism," *Proceedings of the CSEE*, vol. 38, no. 17, pp. 5072-5084, Jun. 2018.

[23] X. Fang, Z. Yang, J. Yu *et al.*, "Theoretical analysis and extension of locational marginal price," *Proceedings of the CSEE*, vol. 40, no. 2, pp. 379-390, Jan. 2020.

[24] Q. Tan, Y. Ding, J. Zheng *et al.*, "The effects of carbon emissions trading and renewable portfolio standards on the integrated wind-photovoltaic-thermal power-dispatching system: real case studies in China," *Energy*, vol. 222, p. 119927, May 2021.

[25] J. Jin, P. Zhou, C. Li *et al.*, "Low-carbon power dispatch with wind power based on carbon trading mechanism," *Energy*, vol. 170, pp. 250-260, Mar. 2019.

[26] Q. Tan, S. Mei, Q. Ye *et al.*, "Optimization model of a combined wind-PV-thermal dispatching system under carbon emissions trading in China," *Journal of Cleaner Production*, vol. 225, pp. 391-404, Jul. 2019.

[27] X. Li, C. Yu, F. Luo *et al.*, "Impacts of emission trading schemes on GENCOs' decision making under multimarket environment," *Electric Power Systems Research*, vol. 95, pp. 257-267, Feb. 2013.

[28] X. Qiao, Z. Yang, Y. Li *et al.*, "Optimization strategy for cooperative operation of multi-microgrids considering two-level carbon trading and demand response," *High Voltage Engineering*, vol. 48, no. 7, pp. 2573-2589, Jul. 2022.

[29] T. Qin, H. Liu, J. Wang *et al.*, "Carbon trading based low-carbon economic dispatch for integrated electricity-heat-gas energy system," *Automation of Electric Power Systems*, vol. 42, no. 14, pp. 8-13, Jun. 2018.

[30] M. Hu, H. Gao, C. Wang *et al.*, "Multiparty co-governance decision-making method for coordinated transactions among multiple microgrids," *Automation of Electric Power Systems*, vol. 46, no. 13, pp. 30-42, Mar. 2022.

[31] D. Xu, B. Zhou, N. Liu *et al.*, "Peer-to-peer multienergy and communication resource trading for interconnected microgrids," *IEEE Transactions on Industrial Informatics*, vol. 17, no. 4, pp. 2522-2533, Apr. 2021.

[32] X. Chang, S. Liu, P. Zhao *et al.*, "Convergent prediction–correction-based ADMM for multi-block separable convex programming," *Journal of Computational and Applied Mathematics*, vol. 335, pp. 270-288, Jun. 2018.

Tao Niu received the B.S. and Ph.D. degrees from the Department of Electrical Engineering, Tsinghua University, Beijing, China, in 2014 and 2019, respectively. He is currently an Assistant Professor with Chongqing University, Chongqing, China. His research interests include voltage security region, automatic reactive power voltage control, renewable generation integration, and reactive power analysis of hybrid AC/DC system.

Haoran Li received the B. S. degree in electrical engineering from China University of Mining and Technology, Xuzhou, China, in 2022. He is currently working toward the M. S. degree with the School of Electrical Engineering, Chongqing University, Chongqing, China. His research interests include multi-microgrid cluster cooperative collaboration and electricity market pricing mechanism.

Guanhong Chen received the B. S. and Ph. D. degrees from Shanghai Jiao Tong University, China, in 2016 and 2023, respectively. He is now working as a Hongshen Young College Teacher of Electrical Engineering Department at Chongqing University, Chongqing, China. His research interests include smart grid, cyber-physical system for power grid, and distributed optimization and control.

Sidun Fang received the B. E. degree from the School of Electrical Engineering, Chongqing University, Chongqing, China, in 2012, and the Ph. D. degree in power system and its automation from the School of Electronics Information and Electrical Engineering, Shanghai Jiao Tong University, Shanghai, China, in 2017. He is currently a Full Professor in Chongqing University. His research interests include integrated energy system and energy-transport integration.

Ruijin Liao received the B.E. degree in electrical engineering from Chongqing University, Chongqing, China, in 1985, the M.E. degree in electrical engineering from Xi'an Jiao Tong University, Xi'an, China, in 1988, and the Ph. D. degree in electrical engineering from Chongqing University, in 2003. He is currently a Full Professor with the School of Electrical Engineering, Chongqing University, and the Vice President of Chongqing University. He is also a Distinguished Professor with Changjiang Scholars of China. He is a Member of GIGRE SC-C4 and CIGRE China National Committee. His research interests include electric breakdown, equipment aging, power transformer, and safety of energy systems.